

Deactivation of vanadia-based commercial SCR catalysts by polyphosphoric acids

Francesco Castellino^a, Søren Birk Rasmussen^{b,1}, Anker Degn Jensen^{a,*},
Jan Erik Johnsson^a, Rasmus Fehrmann^b

^aDepartment of Chemical Engineering, Technical University of Denmark, Building 229, DK-2800 Kgs. Lyngby, Denmark

^bChemistry Department, Technical University of Denmark, Building 207, DK-2800 Kgs. Lyngby, Denmark

Received 7 January 2008; received in revised form 8 February 2008; accepted 13 February 2008

Available online 17 February 2008

Abstract

Commercial vanadia-based SCR monoliths have been exposed to flue gases in a pilot-scale setup into which phosphoric acid has been added and the deactivation has been followed during the exposure time. Separate measurements by SMPS showed that the phosphoric acid formed polyphosphoric acid aerosols, which were characterized by particle number concentrations in the order of $1 \times 10^{14} \text{ \#}/\text{m}^3$ at 350 °C and diameters $<0.1 \text{ \mu m}$. Three full-length monoliths have been exposed to flue gases doped with 10, 100 and 1000 ppmv H_3PO_4 for 819, 38 and 24 h, respectively. At the end of the exposure the relative activities were equal to 65, 42 and 0%, respectively. After exposure, samples of the spent monoliths have been characterized by ICP-OES, Hg-porosimetry, SEM–EDX and in situ EPR. The results showed that the polyphosphoric acids chemically deactivate the vanadia-based catalysts by decreasing the redox properties of the catalyst surface and by titrating the number of V(V) active species. When plate-shaped commercial catalysts have been wet impregnated with different aqueous solutions of H_3PO_4 obtaining P/V ratios in the range 1.5–5, the relative activity for the doped catalysts in the whole P/V range was 0.85–0.90 at 350 °C. These results show that the presence of phosphor compounds in the flue gas may be much more harmful than indicated by simple wet chemical impregnation by phosphoric acid. The reason has been found in the nature of the polyphosphoric acid aerosol formed in the combustion process, which cannot be reproduced by the wet impregnation process.

© 2008 Elsevier B.V. All rights reserved.

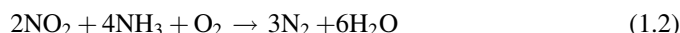
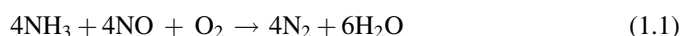
Keywords: SCR catalyst deactivation; Polyphosphoric acid; Vanadia; EPR; SMPS

1. Introduction

Biomass and waste (co)-firing with fossil fuels and NO_x reduction by selective catalytic reduction (SCR) are two practices of increasing application at stationary power stations, which, however, present some economical and technical challenges. Firing of secondary fuels such as biomass, meat and bone meal (MBM), sewage sludge and urban wastes is seen as a way to recover energy while decreasing the net CO_2 emissions. In countries like Denmark and Sweden this practice is forced by local regulations. NO_x emissions are also strictly

limited by national regulations, rendering the utilization of secondary measures like the SCR process necessary.

In the SCR process ammonia is injected into the flue gas and the gas is passed over a catalyst at 300–400 °C [1]. Here the undesired NO_x is reduced to molecular nitrogen according to the following global reactions:



Since NO accounts for roughly 95% of the total NO_x fraction at typical SCR conditions, reaction (1.1) can be considered the dominant SCR reaction.

Commercial catalysts are mainly constituted by vanadium oxide (V_2O_5) supported on a titania (TiO_2) carrier. The total load of V_2O_5 is around 1–5 wt.% depending on the specific application. WO_3 and MoO_3 are also added to the final composition improving both chemical and physical properties

* Corresponding author. Tel.: +45 45 25 28 41; fax: +45 45 88 22 58.

E-mail address: aj@kt.dtu.dk (A.D. Jensen).

¹ Present address: Instituto de Catálisis y Petroleoquímica, CSIC, c/Marie Curie 2, Cantoblanco 28049 Madrid, Spain.

of the catalyst. The catalysts are normally shaped into channels with hydraulic diameters up to 9 mm depending on the fly ash load. A widely accepted mechanism of reaction for these catalysts at typical industrial operating conditions was proposed by Topsøe et al. [2,3]. This involves adsorption of NH_3 on Brønsted acid sites, activation of adsorbed ammonia by $\text{V}=\text{O}$ species and subsequently reaction with gaseous or weakly adsorbed NO.

The SCR technology was first developed and optimized for fossil fuels applications: in the case of pure coal combustion, a catalyst at high dust position has an expected lifetime of up to 5 years. However, when applied at biomass or waste firing the SCR catalysts are reported to experience much faster rates of deactivation [4,5].

Deactivation of SCR catalyst can be due to poisoning, fouling, surface masking, and sintering according to the particular application. Phosphorus is known as a poison for the vanadia-based catalysts. Its poisoning strength was tested in the laboratory both using model $\text{V}_2\text{O}_5\text{--TiO}_2$ and commercial vanadia-based catalysts [6,7]. Generally authors report that poisoning by P is moderate. At 300 °C, a model 5% $\text{V}_2\text{O}_5\text{--TiO}_2$ catalyst wet impregnated with aqueous solution of H_3PO_4 lost about 30% of activity when $P/V = 1$ [6]. Moreover, Kamata et al. [7] found that P is able to some extent to form Brønsted acid sites, which are still able to adsorb ammonia, and could then actively participate in the SCR reaction. Blanco et al. [8] pointed out the negative influence of P on the surface area of vanadia-based honeycomb catalysts extruded with phosphoric acid. However, catalysts extruded with H_3PO_4 and having up to 12.3 wt.% P showed almost the same activity as a P-free catalyst. Beck et al. [9] analyzed SCR catalysts exposed at full-scale plants to flue gases from co-combustion of P-rich fuels (i.e. MBM, sewage sludge) and coal. The catalysts had up to 4.9 wt.% P_2O_5 on the external surface and both a decreased surface area and total pore volume. The authors regarded P as one of the main components responsible for the deactivation of the catalysts and hypothesized the following mechanisms of deactivation by P: (i) poisoning by gaseous P_2O_5 and/or H_3PO_4 ; (ii) pore condensation by polyphosphoric acids; (iii) deposition of alkali phosphates glasses. However, the catalysts were exposed to ill defined conditions and in the presence of other known poisons (e.g. K). Hence it was not possible to clearly point out the main mechanism of deactivation by P and its importance in the simultaneous presence of other deactivating species.

At the time of the writing, the addition of phosphorus compounds to biomass combustion processes is under investigation by Danish power companies [10,11]. It is suggested that this could be an effective measure to reduce the deposition of fly ash on the superheater surfaces, increasing the efficiency of biomass firing. In fact, during biomass combustion the fly ash is rich in K (mainly KCl and K_2SO_4) and has low melting points that make it particularly sticky at the temperatures of the superheater section. Addition of P and Ca has been found to form ashes in the P–K–Ca system with higher melting points and consequently lower tendency to deposit on the superheater exchangers. However, in this case the flue gas

could experience an important increase in total P-concentration [12]. Therefore all the potential drawbacks of this addition process have to be carefully examined at both lab- and pilot-scale, prior to any full-scale applications in the presence of an SCR reactor.

The main objective of this work was to investigate the deactivating effect of P under well defined and realistic operating conditions, thus helping the Danish power companies in foreseeing the potential effects of the P addition process on the SCR catalysts. Full-length commercial SCR monoliths have been exposed for more than 800 h to a flue gas doped with different water solutions of *ortho*-phosphoric acid in a pilot-scale SCR setup. The activity of the monoliths has been periodically tested during exposure and the deactivation mechanisms by P have been pointed out.

2. Experimental

In order to verify the condensation of *ortho*-phosphoric acid and have an online measurement of the activity of a SCR catalyst, a water solution of H_3PO_4 has been injected in a hot flue gas from a natural gas burner. The resulting mixture was then passed over a commercial SCR monolith, and the activity was periodically measured.

2.1. Catalysts

Commercial corrugated-type monoliths and plates obtained from Haldor Topsøe A/S were used in this study. The catalysts were based on V_2O_5 (up to 5 wt.%) and tungsten oxide (WO_3 , up to 9 wt.%) dispersed on a fiber reinforced TiO_2 carrier. The monoliths had a size of 75 mm × 75 mm × 500 mm. The hydraulic diameter of the channels was 6.44 mm and the wall thickness of about 1.0 mm. Pieces of both the fresh and spent monoliths have been cut from both the inlet and the outlet in order to study their local properties under well defined reacting conditions in a laboratory fixed bed reactor. In order to run activity tests on powdered samples, they have been gently crushed in a mortar and the particle fraction in the range 105–125 μm has been collected by sieving. Plate-shaped catalysts were doped with H_3PO_4 at three different levels by a wet impregnation method at room temperature under a vacuum of 0.8 bar absolute pressure to allow the solution to evenly penetrate into the catalyst pores. The catalyst plates had a dimension of 1 mm × 50 mm × 150 mm. They were dried at 120 °C for 1 h and then calcined at 400 °C for 4 h under a stream of 1 L/min of N_2 . The different P/V ratios obtained were measured by inductively coupled plasma optical emission spectroscopy (ICP-OES) and were equal to 1.8, 2.9 and 4.7.

2.2. SCR pilot plant

A schematic of the SCR pilot plant is shown in Fig. 1. The setup runs slightly below atmospheric pressure (5–8 mbar) for safety reasons. Natural gas is burned in the presence of excess air. The flue gas exiting the burner at 950–1000 °C is then led to a high temperature pipe, where the phosphoric acid solution is

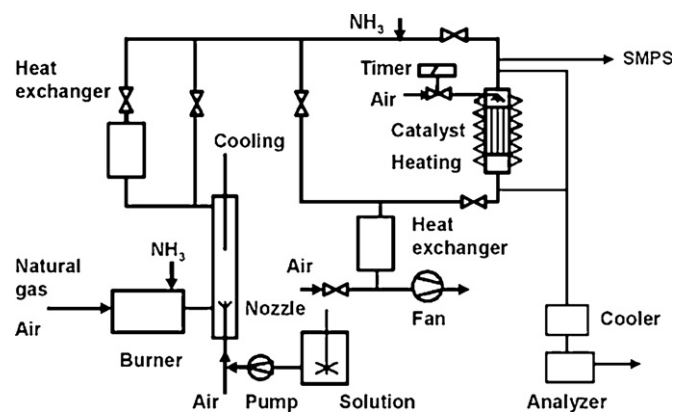


Fig. 1. Schematic drawing of the pilot-scale setup for catalyst monolith deactivation test.

injected. This is done by pumping the desired solution through a water-cooled lance inserted in the high temperature pipe having a two-fluid nozzle at the outlet. Here the water solution meets a flow of compressed air (also added through the lance) and is thus sprayed into the flue gas.

The temperature of the flue gas at the inlet of the SCR reactor can be controlled by adjusting the flow passing through a heat exchanger. For minor adjustments, or simply to avoid that a fraction of the flue gas experiences too low temperature affecting particle condensation rates, the temperature can be controlled by simply adjusting the position of bayonet heat exchanger inserted on the other side of the high temperature pipe. The gas flow is measured by a pitot tube situated at the inlet of the SCR reactor. A throttle valve is used to bypass part of the flue gas and get the desired flow through the reactor.

Ammonia is added into the burner in order to obtain a NO concentration of ~ 500 ppmv at the SCR reactor inlet. If NH_3 was not added, only 80 ppmv of NO would have been present.

The reactor is a squared duct where the catalyst element is vertically supported. In order to have a constant temperature along the whole element, two electric heating wires with temperature control are installed around the reactor. In this way the temperature difference between the inlet and the outlet of the reactor was always kept less than 3°C .

Plate-shaped catalysts have been exposed to the P-rich flue gases by placing them in the pipe downstream the SCR reactor using a squared-plate-holder designed for this purpose.

2.3. H_3PO_4 addition

The addition of H_3PO_4 to the flue gas was performed by spraying different acid water solutions through a nozzle as described above. The solutions were prepared by diluting 85% H_3PO_4 (Fluka Inc.) with distilled water. Three catalyst elements have been exposed to 10, 100 and 1000 ppmv H_3PO_4 . In this work they will be identified by the labels “P10”, “P100” and “P1000”, respectively. The letters “T” and “B” added at the end of the labels will indicate a sample cut respectively from the top (first 5 cm) or the bottom (last 5 cm) of element. In all tests, the solution feed was fixed at 1.25 L/h and the acid concentrations were 0.018, 0.18 and 1.8 mol/L, respectively.

During the 100 ppmv test, five catalyst plates were also exposed. They will be referred as P100plate in this work.

2.4. Activity measurements

The rate of SCR reaction at typical industrial reacting conditions has been assumed to follow an Eley-Rideal mechanism of reaction with NH_3 adsorbed on the catalyst surface and NO reacting from the gas-phase. The following expression for the rate of reaction, r_{NO} , can then be derived:

$$-r_{\text{NO}} \left(\frac{\text{mol}}{\text{m}^3\text{s}} \right) = k_{\text{CNO}} \frac{K_{\text{NH}_3} c_{\text{NH}_3}}{1 + K_{\text{NH}_3} c_{\text{NH}_3}} \quad (1.3)$$

where k (1/s) is the rate constant, c_{NO} and c_{NH_3} (mol/m^3) are the concentrations of NO and NH_3 , respectively, and K_{NH_3} (m^3/mol) is the adsorption constant for NH_3 on the catalyst surface. The fraction term on the right-hand side of Eq. (1.4) is the NH_3 coverage of the catalytic surface, θ_{NH_3} .

At the pilot plant, the activities of the catalysts were measured at 350°C in the presence of about 500 ppmv NO, 600 ppmv NH_3 , 10 vol.% O_2 , 6 vol.% CO_2 , and about 10 vol.% H_2O . During activity measurements (where not stated differently) the flow through the SCR reactor was normally kept at $40 \text{ Nm}^3/\text{h}$. At this flow the gas velocity in the channel was about 6.5 m/s at 350°C , thus similar to the velocities used at full-scale applications, and up to 50% external mass transfer limitations have been estimated.

Since ammonia in our measurements is added in excess with respect to NO (i.e. $\text{NH}_3/\text{NO} \approx 1.2$), the NH_3 coverage, θ_{NH_3} , can be assumed equal to one and the reaction rate can be regarded as pseudo-first order with respect to NO and zero order with respect to NH_3 . Therefore, directly from the fractional NO conversion, X , it is possible to calculate an observed catalyst activity constant, k' , that includes both the influence of external and internal mass transfer:

$$k' \left(\frac{\text{mL}}{\text{g s}} \right) = - \frac{F_{\text{gas}}}{m_{\text{cat}}} \ln(1 - X) \quad (1.4)$$

where F_{gas} is the gas flow rate (mL/s), m_{cat} is the weight of catalyst (g). The degree of deactivation can be then calculated as the ratio k/k_0 between the activity constant of the catalyst during exposure, k , and the one measured for the fresh element, k_0 , right before starting the poison addition.

In the laboratory, powdered samples have been tested for activity in a packed bed quartz micro-reactor with a diameter equal to 10 mm. Around 0.07 g of powder has been used during activity measurement with a total flow equal to $2.8 \text{ NL}/\text{min}$ constituted by 500 ppmv NO, 600 ppmv NH_3 , 5% O_2 and 1.4% H_2O in N_2 . Activity measurements have been performed in the temperature range $250\text{--}400^\circ\text{C}$. The catalyst activity has been calculated according to Eq. (1.5) and the deactivation as the ratio between the activity constant of the spent catalyst and the one measured for the fresh one. At 350°C , the observed activity constant for the fresh catalyst was found only 10% less than the one calculated in the total absence of mass transfer limitations. The latter value was calculated by extrapolating at higher

temperatures the Arrhenius fitting obtained in the range 250–330 °C. No NH_3 oxidation has been measured up to 350 °C during an empty reactor test. In the case of the plates, the activity tests were carried out in another quartz reactor with a diameter equal to 18 mm. The plates were cut into 15 mm \times 15 mm bits. Only one bit, corresponding to around 0.17 g of catalyst, was used for each measurement. This was placed in the center of the reactor and supported by small glass indentations especially designed for the purpose. The total flow and gas composition used during the activity measurements on plates were the same as the ones used for the powders. In previous tests carried out at different flows, it has been shown that when 2.8 NL/min were used, the rate of reaction could be assumed not limited by external mass transfer limitations up to 350 °C.

During all activity measurements, the NO concentration in the dry mixture was measured by conventional UV analyzers (Rosemount NGA 2000).

2.5. Ammonia chemisorption

NH_3 chemisorption is the first step of the reaction mechanism [2,3]. Therefore, NH_3 chemisorption studies have been made to investigate the mechanism of deactivation due to polyphosphoric acid deposition. The tests were carried out in our laboratories using the fixed bed quartz reactor and the catalyst plates. The complete SCR gas mixture described in the previous section was prepared. All the mixture components but NO were then let into the reactor and passed over the catalyst for 30 min. During this time, the catalyst surface got saturated with NH_3 . After this saturation period, the NH_3 addition was shut off and the NO flow was added to the rest of the mixture. Reaction between NO and the previously chemisorbed NH_3 then took place and the amount of NH_3 on the catalyst was calculated from the amount of NO reduced.

2.6. Aerosol measurements

To get a better understanding of polyphosphoric acids formation, aerosols measurements have been carried out at the SCR pilot plant. The particle concentration and size distribution were measured by a Scanning Mobility Particle Sizer (SMPS, TSI Inc.), which included an Electrostatic Classifier (Model 3080) and a Condensation Particle Counter (Model 3775). Particle sampling was carried out at the inlet of the SCR reactor by an ejector sampler running with dry, particle-free air. In this system the particle-containing flue gas was at the same time cooled and diluted. In this way: (i) water condensation was prevented by keeping the sample well above the water dew point; (ii) the rate of coagulation in the sample line was effectively decreased by several orders of magnitude; (iii) overloading of both the impactor and the SMPS was prevented. The dilution ratio, needed to know the real particle concentration in the flue gas, was obtained by measuring the CO_2 concentration both in the flue gas and in the diluted sample. The aerosol measurements were carried out during addition of H_3PO_4 in the range 10–400 ppmv.

2.7. Catalyst characterization

Small pieces of catalyst were cut from the ends of both fresh and exposed monoliths and characterized with respect to bulk chemical composition, mercury porosimetry and physical appearance by a scanning electron microscope (SEM).

The chemical composition was obtained by ICP-OES at the laboratory of DONG Energy A/S and Haldor Topsøe A/S. Prior to the measurements, the samples were cut to 1.5 cm \times 1.7 cm and dried at 105 °C for 2 h before analysis.

The total pore volume and the pore size distribution of the different catalyst sample were made by mercury intrusion in a Micromeritics Autopore II 9220 porosimeter. SEM–EDX analysis was performed at the Teknologisk Institut using a Zeiss Ultra55 and an Oxford ISIS with a Pentafet X-ray detector.

2.8. In situ EPR spectroscopy

Samples (~0.030 g) of both the fresh and the exposed monoliths at the pilot plant (P10 and P100) were placed into a micro-reactor cell specially designed for high temperature EPR measurements using a Bruker ER 4114 HT cavity [13,14]. The spectra were recorded in situ at 350 °C in a flow of around 100 mL/min simulated flue gas. After thermal equilibration, the catalysts were first exposed to a reactant gas composition consisting of 1000 ppmv NO, 3.5% O_2 , 3% H_2O in N_2 . After acquisition of a spectrum at stationary conditions, 1000 ppmv NH_3 was added to the gas mixture. Again after acquisition at stationary conditions, NO was omitted from the reactant gas and the final spectrum was recorded. Spectra were recorded with 1024 points from 2500 to 4500 G, using a time constant of 82 ms and a total sweep time of 84 s. The resonance frequencies were around 9.534 GHz. Modulation frequency and amplitude were 100 kHz and 8.12 G, respectively.

3. Results

3.1. Aerosol measurements at the pilot-scale setup

Table 1 summarizes the main results of the SMPS measurements carried out. In Fig. 2 the particle size distribution (PSD) for the tests with 10, 50, 100 and 400 ppmv of H_3PO_4 are shown. In all the measurements the PSD consisted of only one clear peak. The mean particle size, which was calculated from the total number concentration, was found to vary in the range 25–70 nm and was increasing with the acid concentration in the flue gas. The order of magnitude of the total particle number concentration was equal to 1×10^{14} particles/ m^3 . A blank measurement where only distilled water was sprayed into the setup has also been performed. The results of this measurement showed the presence of particles with a mean diameter equal to 5.81 nm. The total particle number concentration was more than 10 times lower than the one measured when adding 10 ppmv of acid. Table 1 also reports the total P-concentration in the particles measured by the SMPS, together with the ratio between this concentration and the total P injected as H_3PO_4 .

Table 1
Performed SMPS experiments

Experiment		SMPS results			
H ₃ PO ₄ added (ppmv)	P-added (g/m ³)	Particle mean diameter (nm)	Particle total concentration (#/m ³)	P-content (g/m ³)	P-inlet fraction (%)
10	0.006	25.0	3.76E+14	0.003	50
20	0.012	31.8	4.63E+14	0.008	66
30	0.018	36.2	5.20E+14	0.013	72
40	0.024	39.7	5.42E+14	0.018	75
50	0.030	42.8	5.82E+14	0.024	80
70	0.042	46.9	6.30E+14	0.034	81
100	0.061	50.1	6.14E+14	0.041	67
200	0.121	59.4	7.13E+14	0.085	70
300	0.181	63.6	7.63E+14	0.103	57
400	0.243	66.9	8.14E+14	0.127	52

The P-content of the particles has been calculated by assuming the particles at the azeotropic mixture (P₂O₅ = 92.4 wt.%). *T* = 350 °C.

The P-content of the particles has been calculated by assuming the particles constituted by 92.4 wt.% P₂O₅. The reasons for this assumption will be clearer in Section 4.1. The particle density, ρ , has then been calculated as

$$\rho = (0.7102 + 0.01617 \text{ P}_2\text{O}_5 \text{ wt.}\%)T - (11.7E - 4 - 6.00E - 6 \text{ P}_2\text{O}_5 \text{ wt.}\%)T$$

where *T* is the temperature in °C [15]. From the values reported in Table 1, it can be seen that 50–81% of the injected P reaches the catalyst in the particles. Apparently, the mass fraction of P that reaches the inlet of the SCR reactor goes through a soft maximum around 70 ppmv. The remaining may be in the gas-phase or is deposited on the walls of the setup before the catalyst.

3.2. Activity tests at the pilot-scale setup

The three catalyst elements P10, P100 and P1000 have been exposed for 819, 38 and 24 h, respectively. Prior to exposure,

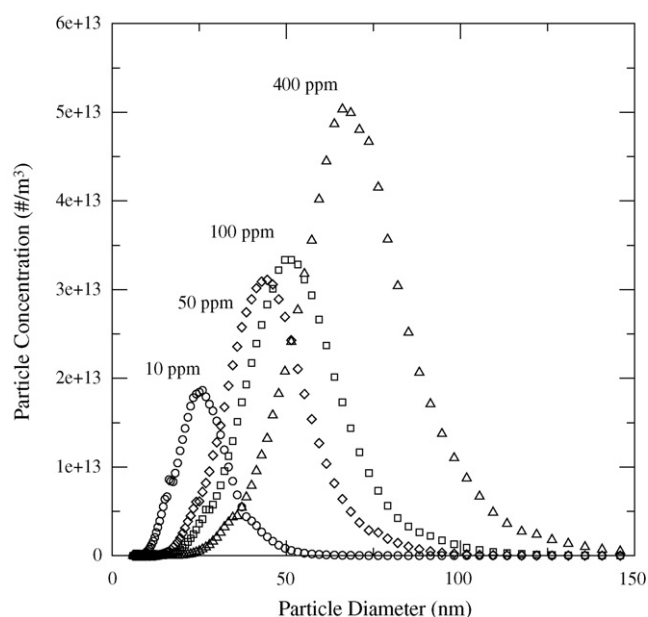


Fig. 2. Particle size distribution of polyphosphoric acids measured at the SCR reactor inlet at different H₃PO₄ addition by SMPS. *T* = 350 °C.

each element has been exposed to a “clean” flue gas for at least 1 week or until its activity had reached a stable value. The different values of activity for the fresh elements have then been used to calculate the relative activity of each catalyst element.

The results of the different deactivation tests are presented in a chronological order.

3.2.1. Exposure to 1000 ppmv H₃PO₄

The addition of 1000 ppmv H₃PO₄ was carried out for 24 h. During the first 2 h of exposure, the activity of the catalyst element was continuously measured. The results of the measurement are shown in Fig. 3. As it can be seen from this, the relative activity rapidly decreased as soon as the P-rich flue gas was flowing through the SCR reactor. After only 2 h the element lost already 33% of its original activity. At the end of the acid addition, the monolith showed no activity at all. The

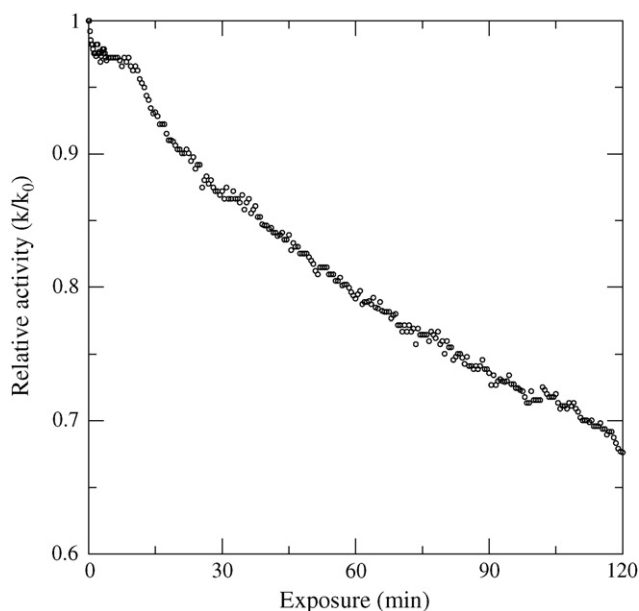


Fig. 3. Relative activity of the P1000 element during the first 2 h of exposure. *T* = 350 °C. Total flow 40 N m³/h. Gas composition on dry basis NO = 496 ppmv, NH₃ = 735 ppmv, O₂ = 10 vol.%, CO₂ = 6 vol.%, N₂ balance. 10 vol.% H₂O.

results show that high level of P in the flue gas may be very harmful to the catalyst.

This test had a tremendous impact on the whole setup. A lot of acid was found deposited on the setup pipe walls and therefore an extensive cleaning was carried out before starting the test at lower acid concentrations.

3.2.2. Exposure to 10 ppmv H_3PO_4

The addition of 10 ppmv H_3PO_4 corresponds to about 32 mg/Nm³ of P_4O_{10} in the flue gas, which is well below the expected P_4O_{10} concentration (3500 mg/Nm³) assuming a 4% co-firing thermal share of sewage sludge with a P-content of 7% and a solid–gas conversion equal to 50% [9]. Fig. 4 shows the decrease in relative activity of the exposed catalyst element. A fresh monolith was charged and exposed to a “clean” flue gas for about 430 h. This time was required in order to get a steady value for the NO conversion. However, the element had already lost about 28% of its original activity, probably due to deposit remaining in the setup even after the cleaning. The addition of 10 ppmv H_3PO_4 was then started. The exposure to the flue gas containing 10 ppmv H_3PO_4 further deactivated the catalyst. However this deactivation was found to be rather slow. Globally, the relative activity leveled off at around 65%, meaning that the element lost 7% of activity since the start of the exposure to 10 ppmv H_3PO_4 . The results indicate that low levels of P in the flue gas may not be very harmful to the catalyst.

During the activity measurements, a transient in the NO conversion was noted when NH_3 was added. This phenomenon was even more evident during the exposure to 100 ppmv H_3PO_4 , and will be therefore presented in the next section.

3.2.3. Exposure to 100 ppmv H_3PO_4

The addition of 100 ppmv H_3PO_4 was carried out for only 38 h. After this time, the element was exposed to a clean flue

Table 2

Results of the activity measurements performed with the P100 element

Operating time (h)	H_3PO_4 addition (h)	X		k/k_0	
		Max	Steady state	Max	Steady state
0	0	0.585	0.585	1	1
20	20	0.569	0.390	0.957	0.562
134	38	0.549	0.312	0.905	0.425
158	38	0.531	0.366	0.861	0.518
180	38	–	0.369	–	0.523
471	38	0.535	0.388	0.871	0.558

gas for additional 433 h. Table 2 reports the activity measurements carried out. During all the measurements, the NO conversion was found to first go through a maximum and then reach a steady level at lower values as a function of time. In Table 2, both the maximum and steady state are reported. Fig. 5 shows the activity measurement carried out after 134 h of operating time. Here, the NO concentration in the flue gas is plotted against the time of the activity measurement. For times less than 0, no ammonia is present in the flue gas and about 514 and 484 ppmv NO are present at the reactor inlet and outlet, respectively. This difference was simply due to dilution of the flue gas with ambient air entering the setup from the pipe flanges. At time 0, around 600 ppmv of NH_3 are added to the flue gas and, as a result of the SCR reaction, the NO concentration starts decreasing until it reaches a concentration of 218 ppmv, corresponding to a NO conversion, X , of 55% and a relative activity, k/k_0 , of 0.91. However, right after reaching this value, the NO concentration in the flue gas starts increasing and reaches a steady-state value at 333 ppmv after about 1 h. In the meantime, the NO concentration at the inlet was measured twice in order to verify that the NO transient was not due to changes in the inlet values. In both cases, this was found equal to about 504 ppmv. This value was only 10 ppmv lower than the initial one and could have been caused by only few degrees change in the burner. At steady state, neglecting the small change in NO inlet concentration, the NO conversion, X , was equal to 0.31, corresponding to a relative activity, k/k_0 , equal to 42%. After having reached the steady state, the amount of NH_3 to the SCR reactor was doubled. Interestingly, the relative activity of the element increased to 50%. Since ammonia is introduced as a pure gas, it is excluded that the drop in NO concentration shown in Fig. 5 is due to dilution of the flue gas. This effect is more likely related to changes in the NH_3 adsorption properties of the P100 surface.

From the analysis of the activity measurements reported in Table 2, it is possible to see that at increasing time of H_3PO_4 exposure, both the maximum and the steady-state value of NO conversion are decreasing. However, when the element was exposed to a H_3PO_4 -free flue gas for some time, it slowly regained some activity. In fact, both the maximum and the steady-state values of NO conversion increased, indicating that part of the deposited acid causing the deactivation is slowly leaving the catalyst.

As it will be discussed later, it is believed that this element is clearly showing effects of chemical deactivation due to

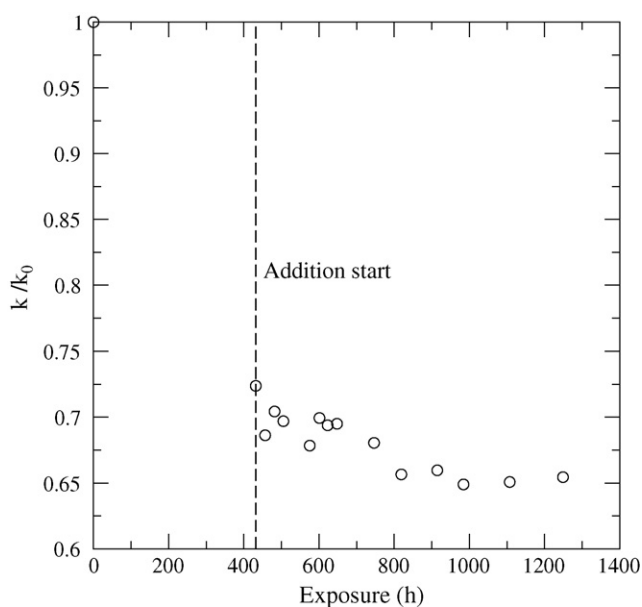


Fig. 4. Relative activity of P10 at 350 °C as a function of exposure time. Total flow 40 N m³/h. Average gas composition NO = 500 ppmv, NH_3 = 735 ppmv, O_2 = 10 vol.%, CO_2 = 6 vol.%, and 10 vol.% H_2O in N_2 .

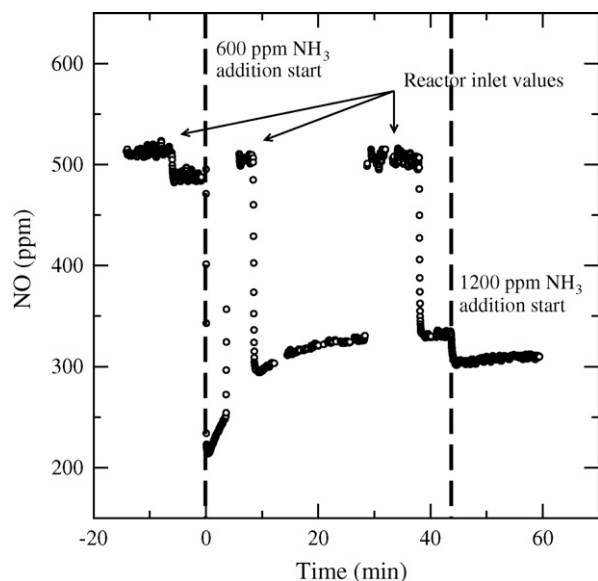


Fig. 5. Activity measurement for P100 at 350 °C and 50 N m³/h after 134 h of operating time. Gas composition on dry basis NO = 515 ppmv, NH₃ = 600–1200 ppmv, O₂ = 11 vol.%, CO₂ = 5.6 vol.%, N₂ balance. 10 vol.% H₂O.

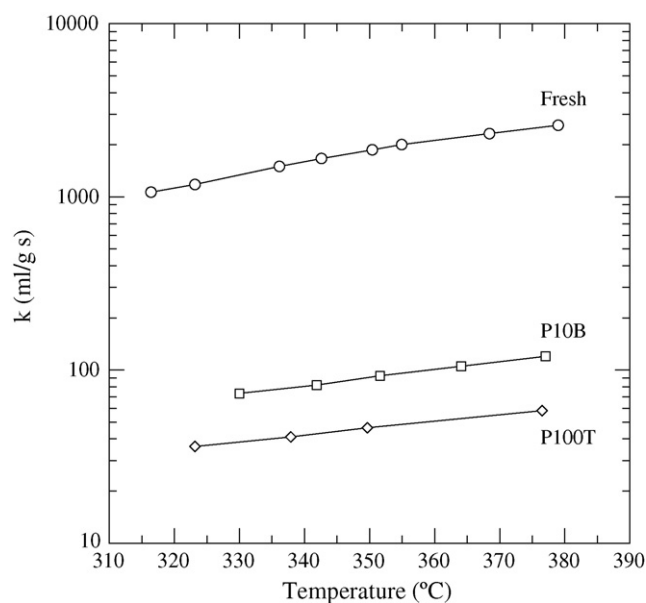


Fig. 6. Activity test on powdered samples. Total flow 2.8 N L/min. NO = 521 ppmv, NH₃ = 622 ppmv, O₂ = 5.2%, H₂O = 1.47%, N₂ balance. Catalyst mass W = 0.072 g.

polyphosphoric acids associated with the transient in NO conversion and due to the formation of V–P–O–NH₃ species, which are not or less active in the reduction of NO than the original sites. Finally, it is worth noting that the NO transient was fully reproducible provided that the NH₃ was shut off for about 1 h. If the element was exposed to an NH₃-free flue gas for shorter times before NH₃ was reintroduced in the flue gas, the NO transient was still present, but the measured maximum NO conversion was lower. This shows that it takes quite some time for the surface complexes to be consumed.

3.3. Lab-scale investigations

3.3.1. Activity tests on catalyst deactivated at the pilot-scale setup

The activity tests on powdered spent and fresh monoliths are shown in Fig. 6. The plot only reports the results in the

temperature range 320–380 °C, where external and internal mass transfer have been estimated not to limit the observed reaction rate. Therefore, the values reported in the plot represent the pseudo-first order intrinsic reaction rate constants. Both the powdered P10B and P100B showed an extreme deactivation: at 350 °C they retained only 5 and 2.6% of their original activity, respectively.

3.3.2. Activity tests on wet impregnated plates

The relative activities of the three different impregnated plates were found in the range 0.85–0.90. Even though the *P/V* ratios (i.e. 1.8, 2.9 and 4.7) for these plates were comparable to the ones measured on the monoliths P10 and P100 (Table 3), their deactivation was much lower, in agreement with other works [6,7] where both model and commercial catalysts have been doped by a wet impregnation method. The results indicate

Table 3
Results of the bulk and surface chemical analysis, and of the Hg-porosimetry for the fresh and spent monoliths.

	Monolith						Plate	
	Fresh	P10T	P10B	P100T	P100B	P1000B	Fresh	P100plate
Bulk chemical analysis								
V (% w/w)	1.60	1.66	2.85	3.12	1.87	0.70	1.00	0.87
P (% w/w)	0.01	3.29	3.02	4.17	4.19	18.70	0.10	6.07
P/V (mol/mol)		3.26	1.74	2.20	2.10	43.94		11.48
Surface chemical analysis								
V (% w/w)	2.1	3.1	3.3	3.9	2.7	1.1		
P (% w/w)	0.0	5.4	4.4	7.9	6.3	21.8		
P/V (mol/mol)	0.0	2.8	2.2	3.3	3.9			
Hg-porosimetry								
Total intrusion volume (mL/g)	0.71	0.57	0.58	0.42	0.53	0.06	0.82	0.44
Total pore area (m ² /g)	36.84	31.16	22.77	19.60	30.67	5.42	73.05	17.19
Catalyst bulk density (g/mL)	0.96	1.15	1.14	1.38	1.17	2.11	0.89	1.20
Porosity (%)	68.60	65.27	66.47	57.73	61.96	11.83	73.02	53.02

that when P does not experience temperatures higher than the calcination temperature used during the doping process, it is not present on the catalyst surface as a polyphosphate. Its deactivating strength is therefore limited.

3.3.3. NH_3 chemisorption tests

Fig. 7 shows the results of the NH_3 chemisorption test performed at 350 °C with a sample cut from P100plate and a fresh plate of the same type. As it can be seen from the plot, the amount of NH_3 adsorbed on the P-deactivated sample was much higher than on the fresh sample. In fact, the P-deactivated sample is able to adsorb about five times more NH_3 than the fresh catalyst. This is in agreement with the increased acidity of the catalyst surface due to deposition of the polyphosphoric acids. However, the activity measurements show that the NH_3 adsorbed on the polyphosphates is much less active (or even non-active), which indicates that in the chemisorption test this NH_3 acts mainly as a reservoir.

3.4. In situ EPR spectroscopy

Fig. 8 shows the in situ EPR spectra of VO^{2+} present on the samples taken from exposure tests of the fresh, P10 and P100 elements measured at 350 °C. Vanadium in oxidation states +5 and +3 are both invisible in EPR at these temperatures. The oxidising mixture NO , O_2 , H_2O in N_2 is leaving the active oxovanadium species present on the catalyst surface mainly in their oxidation state +5. Under these conditions, the spectrum of the fresh catalyst exhibits a broad band from polymeric surface vanadium species. Superimposed on this, a spectrum exhibiting poorly resolved hyperfine structure is observed. The latter appears to be from dimeric V(IV) species, with only the most significant peaks clearly visible. No significant presence of monomeric V(IV) species at this temperature under oxidising

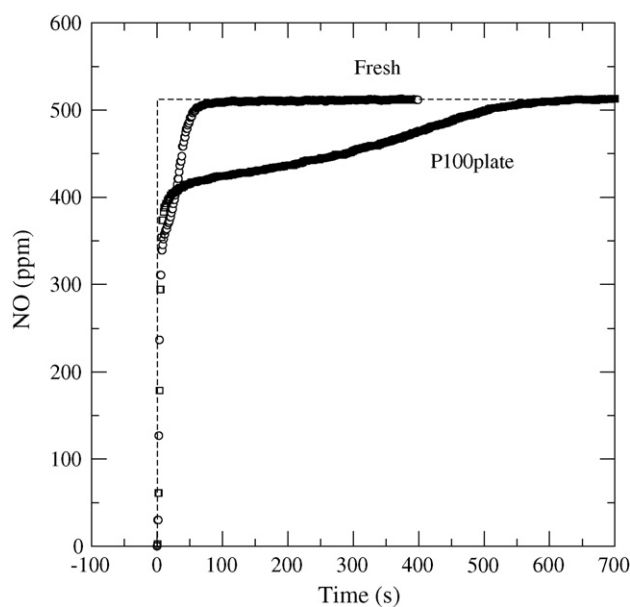


Fig. 7. NH_3 chemisorption test on fresh and P100 mini plate samples at 350 °C. Total flow 2.75 N L/min. NO = 501 ppmv, NH_3 = 601 ppmv, O_2 = 5%, N_2 balance. Catalyst mass W = 0.45 g.

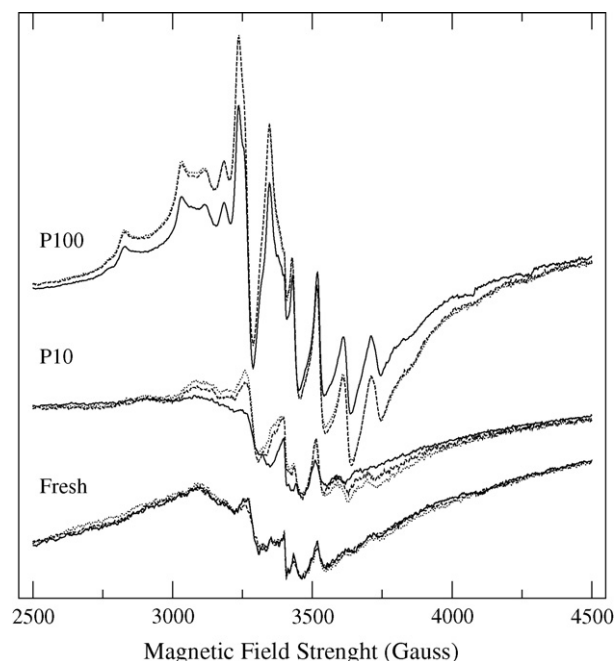


Fig. 8. In situ EPR spectra acquired at 350 °C of catalyst samples taken from pilot plant tests fresh, P10 and P100, exposed to various simulated flue gas compositions. Gas composition: 1000 ppmv NO (—), 1000 ppmv NO + 1000 ppmv NH_3 (···), 1000 ppmv NH_3 (- - -) and 3.5% O_2 , 3% H_2O in N_2 .

conditions is observed. During exposure to NH_3 -containing gases, the redox chemistry of the fresh catalyst surface is not altered at all, as shown by the identical spectra, which were recorded during exposure to the different gas mixtures.

The P10 sample essentially shows the same spectrum as the fresh catalyst after equilibration in the oxidising NO , O_2 , H_2O , N_2 atmosphere. However, unlike the uncontaminated sample, the exposure to an NH_3 -containing mixture caused an increase in VO^{2+} (or $(\text{VO}^{2+})_n$) content. In particular, the spectrum of the sample equilibrated in the SCR gas mixture exhibited the greatest difference from oxidising conditions.

Contrarily to the previous results, P100 showed a significantly increased broad band of polymeric $(\text{VO}^{2+})_n$ species even during exposure to the oxidising gas mixture. Superimposed on this signal, a new but recognisable contribution from monomeric VO^{2+} species is observed.

3.5. Catalyst characterization

The V- and P-content on both the surface and bulk of the fresh and doped catalyst are shown in Table 3. The results of the mercury porosimetry are also reported in Table 3. In all the tested cases, the P-levels in the bulk were found slightly higher at the inlet compared to the outlet of the catalyst element, according to both the higher particle concentration and the higher mass transfer due to the developing flow and higher level of turbulence.

The P-content of the P100 element was found slightly higher than the one measured for the P10 (i.e. about 4 wt.% against 3 wt.%). Considering the big difference in exposure time for the two experiments (819 h vs. only 38 h), and assuming a linear

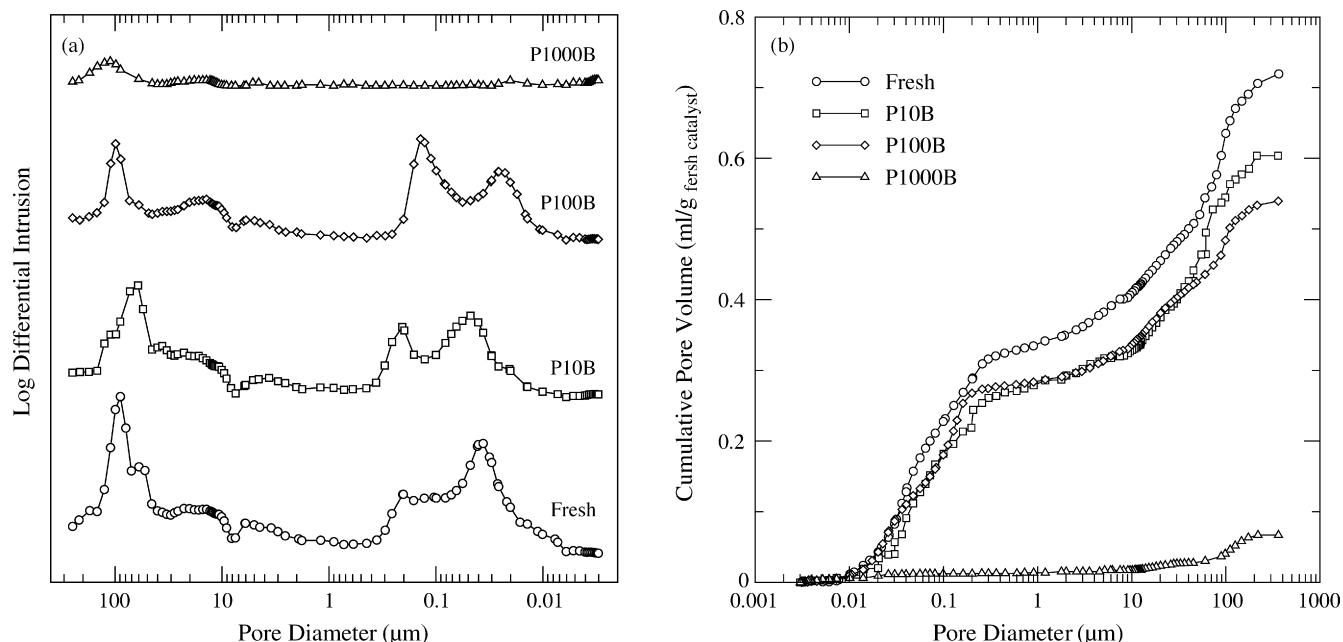


Fig. 9. Pore size distribution and cumulative intrusion volume measured by Hg-porosimetry with different monolithic samples.

and constant deposition of P vs. time, it can be calculated that the overall accumulation rates have been 0.09%/day and 2.6%/day for P10 and P100, respectively. Assuming a first order process for the particle deposition (i.e. the fraction of deposited particles not depending on the total particle concentration number) and making the conservative assumption that the particle formed during the addition of 10 ppmv H_3PO_4 have the same diffusivity of the bigger particles formed in the presence of 100 ppmv H_3PO_4 , the deposition rate for the 100 ppmv H_3PO_4 test should have been only 10 times higher than the one with 10 ppmv H_3PO_4 . As calculated before, the P-accumulation on P100 was instead found 29 times the P-accumulation on P10. This fact, as it will be discussed later, is considered as an indication that the overall P-accumulation is the result of a balance between particle deposition and deposit hydrolysis followed by P-vaporization from the sample.

According to the results obtained by Hg-porosimetry shown in Fig. 9, the deposition of polyphosphoric acid produced a shift toward smaller pore diameters in the pore size distribution for the different monoliths, pointing out the occurrence of physical deactivation due to pore blocking and condensation. In fact, it appears that the smaller pores at 40–50 nm of the bimodal mesoporous system are filled during P-addition, and a partial blocking of the interparticulate pore structure happened for P10 and P100. Furthermore, large crystalline formation has filled the void space in the macro-cracks above 100 μm. For the P10 a shift towards smaller macropores is observed due to this, whereas for the P100, a more dispersed destruction of the entire pore system is observed.

Overall, the total intrusion volume (TIV) was found to decrease at increasing P-content (Fig. 10).

The physical deactivation pointed out by the Hg-porosimetry measurements has also been confirmed by SEM analysis of the exposed catalysts (Fig. 11). From these it can be seen that

the surface of P100 looks uniformly covered by a glassy layer, whereas the porous structure of titania is more defined on the surface of P10. Instead, on this latter, some needle-shaped crystals are present. The analysis of these crystals by EDX showed enrichment in both P and V.

Fig. 12 shows the distribution of P into the walls of P10B and P100B as measured by EDX at the points shown in Fig. 11. P was found to penetrate the whole catalyst wall in both cases. In particular, the P-content in P100B was found constant around a value of 6.1 wt.%. Differently, the concentration profile measured on P10B showed a gradient in P-concentration in

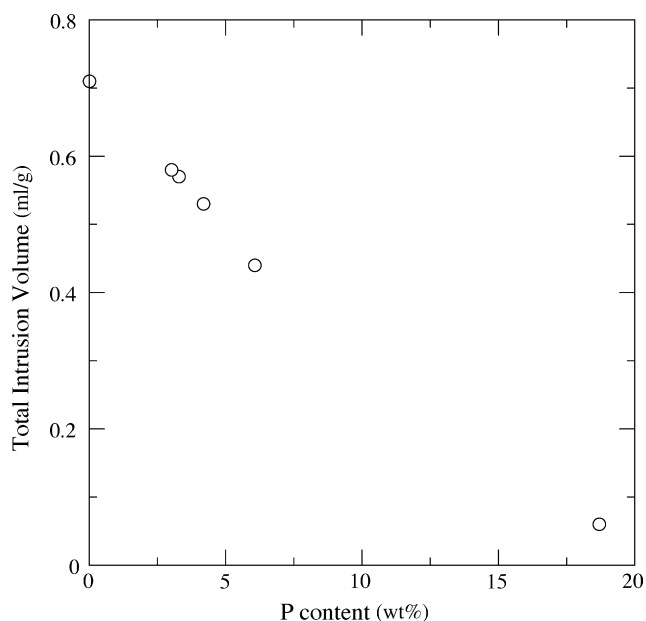


Fig. 10. Total intrusion volume measured by Hg-porosimetry as a function of P-content measured in the bulk of the different spent monoliths.

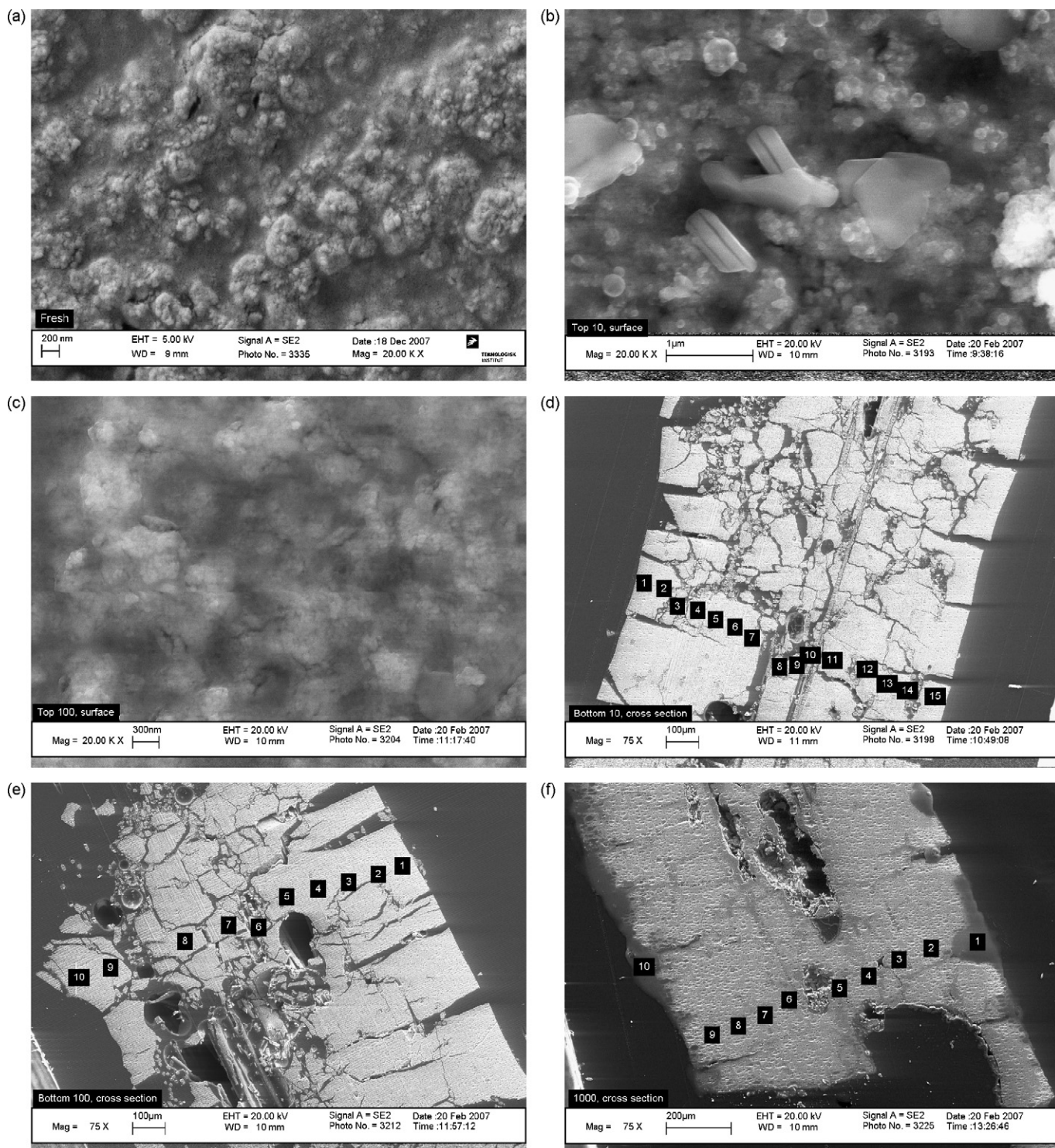


Fig. 11. SEM analysis of fresh and spent catalyst: (a) fresh surface; (b) P10T surface; (c) P100T surface; (d) P10B wall cross-section; (e) P100B wall cross-section and (f) P1000B wall cross-section.

the proximity of the surface, normally indicating a diffusion limited process in P-accumulation. However, in some points in the middle of the wall, especially in the proximity of a macropore, the P-concentration was found again higher. Overall, the average P-content in P10B wall was equal to 3.1 wt.%.

4. Discussion

A higher degree of deactivation was obtained by exposure to polyphosphoric acid aerosols at the pilot plant compared to the one obtained by wet impregnation of H_3PO_4 aqueous solutions. This indicates the importance in understanding the mechanism

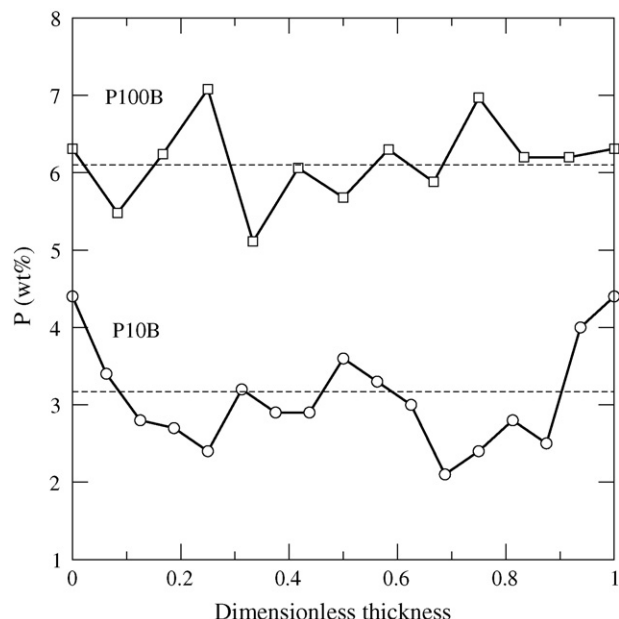


Fig. 12. P-content measured by EDX across some catalyst walls shown in Fig. 11.

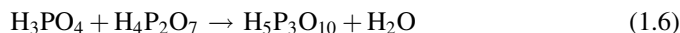
of formation of these particles and their influence on the activity of the vanadia-based catalysts. Apparently the real poisoning strength of P is not reproduced by the wet impregnation method normally used to dope both model and commercial catalysts.

4.1. Polyphosphoric acids formation and deposition

The measured particles had very small mean diameters and a total particle number concentration in the order of $1 \times 10^{14} \text{ \#}/\text{m}^3$ indicating their formation by homogeneous nucleation from the gas-phase. Condensation on particles already present (i.e. the ones measured during the blank measurement) cannot be completely excluded. However, this cannot be regarded as the main mechanism of particle formation since already at the lower acid concentrations (i.e. 10 ppmv), the particle number concentration was more than 10 times higher than the one found during the blank test. Furthermore, due to the very small size of the particles measured during the blank test, their mass fraction in the deposits can be neglected.

In order to explain the particle formation experienced, the formation of polyphosphoric acid will be here discussed based on Ref. [16]. The phosphoric acid molecule H_3PO_4 can be written as $1/2\text{P}_2\text{O}_5 \cdot 3\text{H}_2\text{O}$ and thus be considered as a 72.5% P_2O_5 solution having a boiling point temperature at 255°C . When exposed to higher temperatures, water can evaporate until an azeotropic mixture consisting of 92.4% P_2O_5 is formed. This azeotropic mixture has a much higher boiling point at 864°C . This water evaporation and the subsequent increase of P_2O_5 concentration is the result of condensation reactions taking place between the H_3PO_4 molecules in the gas-phase producing chains of poly-, pyro-, tri-, and *meta*-phosphoric acid, as

follows:



Due to their higher boiling point temperatures, the polyphosphoric acids may condense according to their vapor pressure when the gas cools down to the SCR reactor temperature.

Fig. 13 shows a plot of the partial pressure of different polyphosphoric acids as a function of P_2O_5 content [17]. Since particles have been found at the reactor inlet even at the lowest acid concentration of 10 ppmv, and considering the high temperatures ($>850^\circ\text{C}$) experienced in the spraying section of the setup, it is assumed that the composition of the deposited particles is equal to the azeotropic mixture. In this way, around 50–81% of the injected P-mass, was collected at the inlet of the SCR reactor. In the absence of a direct measurement of the P-content in the gas-phase, it is difficult to completely exclude and/or quantify the presence of gaseous P-species at the reactor inlet. Considering the equilibrium between the gas- and the liquid-phase as described by Fig. 13, no condensation with 10 ppmv H_3PO_4 is expected since this would have needed a supersaturated atmosphere in order to take place. However, this was not the case. Moreover, the fraction of P calculated from the particle number concentration measured by the SMPS was found in the range 50–81%. If it is assumed that at low acid concentrations the rest of the injected P is in the gas-phase, this should have been close to zero at increasing acid concentrations. However, as shown in Table 1, the collected P-fraction at 400 ppmv H_3PO_4 was almost the same as the one at 10 ppmv.

It is therefore assumed that: (i) the injected H_3PO_4 reacted in the gas-phase forming an azeotropic mixture of polyphosphoric

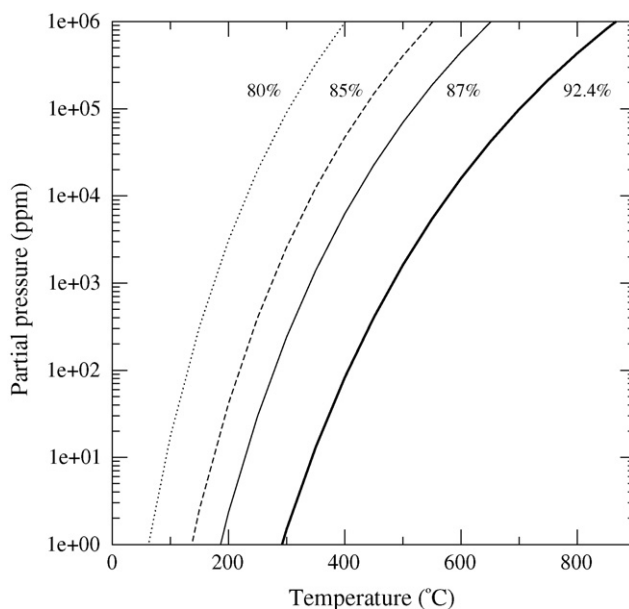


Fig. 13. Vapor pressure of polyphosphoric acids as a function of temperature at different P_2O_5 weight content. The lines are calculated by extrapolating at lower pressures the equation fitting the experimental data found at higher partial pressures [17].

acids; (ii) nucleation of polyphosphoric acid happened at temperatures $<500\text{ }^{\circ}\text{C}$; (iii) almost all the acid was present in the liquid-phase and (iv) the differences found between the total P-mass injected and the P-mass measured at the SCR reactor inlet was mainly due to particle deposition on the pipe walls leading to the SCR reactor.

Due to their submicron dimensions, the particles are very mobile and can diffuse towards the catalyst walls, deposit on the catalyst surface and even penetrate into the pore structure by capillary forces. Once deposited, however, some of the deposited polyphosphoric acid may be hydrolyzed in the presence of the flue gas moisture forming H_3PO_4 which evaporates from the catalyst. The resulting P-accumulation rate is therefore a balance between the particle deposition and evaporation of phosphoric acid. The hydrolysis of polyphosphoric acid in water is known to be a slow process and dependent on different factors, such temperature, chain length and pH [16]. Therefore the P-accumulation in the catalyst walls will be mainly controlled by the particle deposition rate at high total particle numbers, while deposit evaporation at low deposition rates and low total particle number concentrations becomes relatively more important.

Taking into account all these facts, together with the different P-concentration profiles measured by EDX on P10 and P100 (Fig. 12), it is possible to conclude that evaporation of phosphorus compounds effectively limited the P-accumulation in the P10 case and that the profile measured in the wall is the net result of deposition and evaporation. The deposition rate during the 100 ppmv H_3PO_4 addition was much faster than evaporation leading to a fast accumulation of P in the wall.

4.2. Deactivation mechanisms

The high P-concentration found in the bulk of the exposed catalysts, the even P-distribution measured along the catalyst walls, the decrease in TIV measured by Hg-porosimetry at increasing P-concentrations and the SEM analysis of the different catalyst surfaces, all point to the occurrence of physical deactivation due to surface masking, pore blocking and condensation, in agreement with previous investigations about P-deactivation. However, the transient in NO conversion observed during every activity measurements clearly points out the occurrence of a simultaneous chemical deactivation mechanism.

The in situ EPR measurements carried out with the fresh catalysts have shown that the different gas compositions are not able to change the redox properties of the surface. In particular, during the SCR reaction, the V(V) species are continuously reduced during formation of the reaction intermediates and then re-oxidised by O_2 [2,3]. The fact that this sample, when exposed to the complete SCR mixture, does not show an increased number of V(IV) species can be explained assuming that at $350\text{ }^{\circ}\text{C}$ the rate of re-oxidation of the active V(IV) species in the redox cycle of the mechanism is high enough to keep the vanadium as V(V). In other words, this behaviour confirms the literature consensus [1] that at this temperature, the order of reaction of oxygen is zero.

Under oxidising conditions, P10 practically exhibited the same spectrum as the fresh sample. However, when P10 was exposed to the complete SCR gas mixture, the number of $(\text{VO}^{2+})_n$ species slightly increased. This indicates that the SCR reaction is occurring, but that the re-oxidation step is significantly slower than for the fresh catalyst.

Contrarily to the previous results $(\text{VO}^{2+})_n$ species are present as a stable phase on the catalyst surface of the P100 sample already under oxidising conditions, suggesting that the VO^{2+} on P10 and P100 are exposed to two distinctly different phosphor species. Furthermore, the concentration of V(IV) is increased when NH_3 is added to the mixture and the SCR reaction takes place. The most likely explanation for this is that the intermediate V(IV) species, which are consistently formed during the SCR reaction [2,3], are being trapped by phosphate interactions, since it appears unlikely that phosphates alone should be able to reduce the V(V) compounds. This indicates that the deposited phosphates interact with parts of the active oxo-vanadium species, forming vanadyl-phosphate species which will not take part in the reaction anymore, thus inducing chemical deactivation by titration of the active species.

By considering this chemical deactivation, together with the effect of intra-particle diffusion limitations, the transient in NO conversion can be explained. As shown in Fig. 5, at the very beginning of the NH_3 addition, the monolith P100 still presents a relative good activity. As reported in Table 2, when the NO conversion goes through the maximum, the relative activity is equal to 0.91. The lost 9% of activity is mainly due to physical deactivation only. However, the V(IV) species which were initially formed during the SCR reaction, are then stabilized in complexes which are formed with the deposited polyphosphoric acids. NH_3 can then be considered as the responsible for this titration of active sites since it initiates their reduction due to the SCR reaction. This titration is assumed to happen first at the outer catalyst wall, since it is where the SCR reaction is first happening. The intrinsic rate of reaction then starts decreasing at the outer wall due to the formation of $\text{NH}_3\text{-P-V}$ species and the reagents have to diffuse further into the catalyst walls in order to find active sites where to react. The steady-state is finally reached when equilibrium between the formed P-V-complexes, the active V-species and NH_3 is reached along the catalyst wall. In the case shown in Fig. 5 and reported in Table 2, the additional 48% of activity which has been lost has to be considered due to chemical deactivation.

NH_3 is controlling the stability of the formed and inactive complexes. In fact, the NO transient during the activity measurement can only be reproduced if NH_3 has been taken off the flue gas for the time required by these complexes to completely disappear. Moreover, as shown in Fig. 5, further NO conversion can be obtained by increasing the NH_3 partial pressure, but again this will first show a maximum and then a steady-state level at lower values. This additional activity at higher NH_3 partial pressures can be related to the NH_3 adsorption constant of the catalyst surface, which is changed due to the presence of the polyphosphoric acids. As shown in Fig. 7, the amount of chemisorbed NH_3 is increased due to the polyphosphoric acid deposition. However this additional

adsorbed NH_3 can be assumed either *less active*, in agreement with Kamata et al. [7], or inactive, simply constituting an NH_3 storage on the surface. In the latter case, it has first to jump on an active site prior to react. Regarding the increased activity, which was measured when the NH_3 concentration was increased, it can then be argued that, due to the increased number of sites for the NH_3 chemisorption, the coverage of NH_3 appearing in Eq. (1.4) has become less than one at the typical condition of our activity measurements.

Finally, the reason for P100 for showing a more pronounced transient than P10 has to be found in: (i) a higher P-content in P100 and a consequent slower diffusivity due to the decreased pore sizes; (ii) a higher degree of polymerization of the deposits in P100 due to the faster deposition compared to the hydrolysis rate; (iii) a more uniform distribution of P in the P100 walls.

5. Conclusions

When exposed to the high temperatures of a combustion process, the H_3PO_4 molecules eventually released in the gas-phase start condensation reactions forming polyphosphoric acids. These species are characterized by higher melting point temperatures than the typical SCR reaction temperatures and are found in a liquid-phase at the SCR reactor inlet. Condensation of these species has been estimated to happen at temperatures lower than 500°C . Therefore, there is a high probability that the formed aerosols will be characterized by high number concentrations of submicron liquid particles, due to the short time passing between the nucleation burst and the SCR reactor inlet. These particles therefore have high diffusivities and a high deposition rates on the monolith walls.

Deactivation by polyphosphoric acid has been found to follow both a physical and a chemical deactivation. Surface masking, fouling, pore blocking and condensation are definitely important contributions to catalyst deactivation. Once deposited on the catalyst outer surface, they are very mobile and can even be sucked into the walls by capillary forces. The P-accumulation, and consequently the implied deactivation, is however limited by the rate of hydrolysis of the deposits themselves. The H_2O present in the flue gas, at the SCR temperatures can break down the polyphosphoric acid chains and free some H_3PO_4 back in the gas-phase.

The physical deactivation, however is not the only effect responsible for the overall measured deactivation levels. Supported by the transient behaviour in NO reduction measured during activity tests with mass transfer-limited-catalysts, and in situ EPR analysis of the spent catalysts, it has been found that the deposited polyphosphoric acids tend to both increase and stabilize the number of *non-active* V(IV) species, which are formed as intermediate during the SCR reaction. Moreover, part of the NH_3 present in the gas-phase preferentially adsorbs

on the polyphosphoric acids and is only less active in the reduction of NO.

The results obtained in this work constitute the first reference about deactivation of vanadia-based catalysts explicitly due to polyphosphoric acid alone. It is believed they show the real deactivating potential of P, when this is present in the flue gas during post-treatment of combustion processes, which has been found much more poisonous than indicated by wet impregnated tests.

Acknowledgments

This work is part of the CHEC (Combustion and Harmful Emission Control) Research Center funded a.o. by the Technical University of Denmark, the Danish Technical Research Council, the European Union, the Nordic Energy Research, Dong Energy A/S, Vattenfall A.B., F L Smidth A/S, and Public Service Obligation funds from Energinet.dk and the Danish Energy Research program. In particular, it is supported by the PSO project “Deactivation of SCR Catalysts by Additives” (PSO Elkraft FU-4205). Supply of the catalyst samples by Haldor Topsøe A/S is gratefully acknowledged.

References

- [1] V.I. Parvulescu, P. Grange, B. Delmon, *Catal. Today* 46 (1998) 233–316.
- [2] N.-Y. Topsøe, H. Topsøe, J.A. Dumesic, *J. Catal.* 151 (1995) 226–240.
- [3] N.-Y. Topsøe, J.A. Dumesic, H. Topsøe, *J. Catal.* 151 (1995) 241–252.
- [4] Y. Zheng, A.D. Jensen, J.E. Johnsson, *Appl. Catal. B: Environ.* 60 (2005) 261–272.
- [5] Y. Zheng, A.D. Jensen, J.E. Johnsson, *Appl. Catal. B: Environ.* (2008), doi:10.1016/j.apcatb.2008.02.019.
- [6] J.P. Chen, M.A. Buzanowski, R.T. Yang, *J. Air Waste Manage. Assoc.* 40 (1990) 1403–1409.
- [7] H. Kamata, K. Takahashi, C.U.I. Odenbrand, *Catal. Lett.* 53 (1998) 65–71.
- [8] J. Blanco, P. Avila, C. Barthelemy, A. Bahamonde, J.A. Odriozola, J.F. Garcia de la Banda, H. Heinemann, *Appl. Catal.* 55 (1989) 151–164.
- [9] J. Beck, J. Brandenstein, S. Unterberger, K.R.G. Hein, *Appl. Catal. B: Environ.* 49 (2004) 15–25.
- [10] P.A. Jensen, L.H. Sørensen, G. Hu, J.K. Holm, F. Frandsen, U.B. Henriksen, Technical University of Denmark, KT-Report No. 0504, 2005.
- [11] L. Tobiasen, R. Skytte, L.S. Pedersen, S.T. Pedersen, M.A. Lindberg, *Fuel Process. Technol.* 88 (2007) 1108–1117.
- [12] J. Beck, R. Muller, J. Brandenstein, B. Matschenko, J. Matschke, S. Unterberger, K.R.G. Hein, *Fuel* 84 (2005) 1911–1919.
- [13] K.M. Eriksen, R. Fehrmann, N.J. Bjerrum, *J. Catal.* 132 (1991) 263–265.
- [14] M.Y. Kustova, S.B. Rasmussen, A.L. Kustov, C.H. Christensen, *Appl. Catal. B: Environ.* 67 (2006) 60.
- [15] T.D. Farr, *Phosphorus Properties of the Element and Some of Its Compounds*, Tennessee Valley Authority, Chemical Engineering Report No. 8, U.S. Government Printing Office, Washington, DC, 1950. From <http://www.innophos.com>.
- [16] J.R. Van Wazer, *Phosphorus and its Compounds*, Interscience Publisher, New York, 1958.
- [17] E.H. Brown, C.D. Whitt, *Ind. Eng. Chem.* 44 (1952) 615–618.